

7-8-1992

Functional and Morphological Studies of Mitochondria Exposed to Undecagold Clusters: Biologic Surfaces Labeling with Gold Clusters

E. Valdivia
University of Wisconsin, Madison

C. Gabel
University of Wisconsin, Madison

J. E. Reardon
University of Wisconsin, Madison

C. A. CaJacob
University of Wisconsin, Madison

H. Yang
University of Wisconsin, Madison

Follow this and additional works at: <https://digitalcommons.usu.edu/microscopy>

 [Part of the Biology Commons](#) [next page for additional authors](#)

Recommended Citation

Valdivia, E.; Gabel, C.; Reardon, J. E.; CaJacob, C. A.; Yang, H.; Wehbi, R. S.; Scott, G. L.; Frey, P. A.; and Fahien, L. A. (1992) "Functional and Morphological Studies of Mitochondria Exposed to Undecagold Clusters: Biologic Surfaces Labeling with Gold Clusters," *Scanning Microscopy*. Vol. 6 : No. 3 , Article 15. Available at: <https://digitalcommons.usu.edu/microscopy/vol6/iss3/15>

This Article is brought to you for free and open access by the Western Dairy Center at DigitalCommons@USU. It has been accepted for inclusion in Scanning Microscopy by an authorized administrator of DigitalCommons@USU. For more information, please contact digitalcommons@usu.edu.



Functional and Morphological Studies of Mitochondria Exposed to Undecagold Clusters: Biologic Surfaces Labeling with Gold Clusters

Authors

E. Valdivia, C. Gabel, J. E. Reardon, C. A. CaJacob, H. Yang, R. S. Wehbi, G. L. Scott, P. A. Frey, and L. A. Fahien

FUNCTIONAL AND MORPHOLOGICAL STUDIES OF MITOCHONDRIA EXPOSED TO UNDECAGOLD CLUSTERS: BIOLOGIC SURFACES LABELING WITH GOLD CLUSTERS

E. Valdivia*, C. Gabel, J.E. Reardon, C.A. CaJacob, H. Yang,
R.S. Wehbi, G.L. Scott, P.A. Frey and L.A. Fahien

Departments of Pathology, Pharmacology, Preventive Medicine,
Anatomy, Biochemistry, Enzyme Institute and Integrated
Microscopy Resource, University of Wisconsin, Madison

(Received for publication October 18, 1991, and in revised form July 8, 1992)

Abstract

This study reports morphological and functional alterations observed in respiring isolated mitochondria when they are exposed to nonpenetrating, positive electrostatically charged synthetic undecagold clusters. Modification of the undecagold clusters positive charges change or prevent the functional effects and the binding to the outside surface of the mitochondria. The mitochondrial functional alterations are dependent on the oxidative phosphorylation capacity of the isolated organelles. The results of these experiments indicate that artificial undecagold may be useful to explore the molecular mechanisms of biological energy transducers which require electric charges separation, ionic fluxes, and electric surface properties.

Key Words: gold cluster, undecagold cluster, gold labeling, electron microscopy, electron dense probes, mitochondria, enzyme, respiratory control, oxygen consumption, macromolecules.

*Address for correspondence:

E. Valdivia
Depts. Preventive Medicine & Pathology,
Univ. of Wisconsin,
502 N. Walnut, Madison, WI 53705-2368
Phone No.: [608] 262-0418

Introduction

The experiments described in this paper demonstrate morphological and functional alterations induced on isolated respiring heart mitochondria by synthetic undecagold made to exhibit positive electrostatic charges. These studies are important because they explore molecular mechanisms of energy transduction localized in mitochondria and dependent on electron charge separation (Mitchell, 1966). Transduction of energy is a vital biological process represented in organisms by photosynthesis and by oxidative phosphorylation. The energy requirements of the cells correlate well with mitochondrial populations seen by electron microscopy: fetal liver cells have fewer mitochondria than adult liver (Lehninger, 1970; Valcarce *et al.* 1990). Correlation between oxygen uptake and mitochondrial volume has been demonstrated in mammalian skeletal muscle (Hoppeler, 1990). Proliferation and enlargement of mitochondria has been shown in guinea pigs living at low barometric pressures (Valdivia *et al.*, 1960). The regulation of mitochondrial oxidative phosphorylation has been extensively studied in organs, cells and isolated organelles; more recent literature reviews are presented by Balaban *et al.* (1990), From *et al.* (1990), and Moreno-Sanchez *et al.* (1990).

The isolation of mitochondria and their fragmentation has led to the experimental exploration of the mechanisms responsible for oxidative phosphorylation at the membrane organelle level by Crane *et al.* (1956), Chance and Williams (1956), Hackenbrock (1972), Jacobus *et al.* (1982) and more recent studies are reviewed by Hatefi (1985). Lardy and Wellman (1953) interpreted the ADP stimulation of isolated liver mitochondrial respiration to be the acceptor control mechanism regulating oxidative phosphorylation. Chance and Williams (1956) extended these studies and correlated the kinetic influence of substrates, oxygen and production of ATP to metabolic states characteristic of functional mitochondria suggesting that functional and structural integrities of these organelles are reflected by the respiratory control rates which are influenced mainly by ADP present in the medium. A thermodynamic mechanism explaining respiratory control has been proposed by

Erecinska and Wilson (1982). Mitchell's chemiosmotic hypothesis (1966) proposed that regulation of respiratory control is based in the variability of electromotive forces at the mitochondrial membrane. Experiments on intact animals and isolated organs suggest that mitochondrial respiration is a function of the availability of substrates entering into the electron transport chain (Heineman and Balaban 1990).

The objectives of this report are: first, to describe a stimulation of respiration in well-coupled, heavy beef heart mitochondria (HBHM) after their exposure to synthetic undecagold cluster made to have 21 peripheral positive charges, gc 21+. Second, to describe the morphologic changes produced by gc 21+ binding to uncoupled HBHM and light beef heart mitochondria (LBHM). Third, to report functional alterations induced by gc 21+ on the different types of heart mitochondria and fourth, to demonstrate morphologic changes induced by gc 21+ on mitochondrial membranes and enzymatic complexes dependent on electrostatic charges and binding.

The reason macromolecules with positive surface electrostatic charges influence mitochondrial structures and function is because the probes positive charges compensate and bind to the negative charges developed on the respiring organelles. The exact molecular mechanism responsible for the experimentally demonstrated charges separation is not known but arguments are described by Mitchell (1966). We selected undecagold clusters and cationized ferritin because they are easily available and we could synthesize modified artificial probes at our discretion. Furthermore, both probes can be quantized. The binding of cationized ferritin to the outside of the outer membrane produces similar effects as the positively charged undecagold clusters indicating that the positively charged probes do not penetrate into the inner compartments when included in experiments as described in these studies which suggests that there must be an indirect signal type of mechanism between the external membrane and the inner mitochondrial membrane.

Abbreviations

ADP:	adenosine 5'-diphosphate
ATP:	adenosine 5'-triphosphate
DNP:	dinitrophenol
EDAX:	energy dispersive analysis of X-rays
EDTA:	ethylene diamine-tetraacetic acid
EGTA:	ethylene (glycol-bis-betaaminoethyl ether)NNN1N1 tetraacetic acid
ETPH:	electron transport particles, heart
gc:	gold cluster
gc 21+:	gold cluster with 21 +ve charges at pH 7
HBHM:	heavy beef heart mitochondria
La:	Lanthanum
LBHM:	light beef heart mitochondria
TEM:	transmission electron microscopy
Tris:	Tris(hydroxymethyl)aminomethane
Pi:	inorganic phosphate
PTA:	phosphotungstic acid

Materials and Methods

Electron dense labels. Synthesis of gold cluster with 21+ charges (gc 21+)

The method of preparation and many properties of gold clusters were reported by Cariati and Naldini (1971) and by Albano *et al.* (1970) (Figure 1). Bartlett *et al.* (1978) described a method to synthesize gc 21+ by borohydride reduction of an alcoholic solution of equimolar aureous cyanide and the phosphine ligand. Concentrations of gc 21+ in solutions and its binding to macromolecules and organelles were calculated by measuring absorbance at 415 wavelength assuming an extinction coefficient of $2.95 \times 10^4 \text{ M}^{-1} \text{ cm}^{-1}$ (Reardon and Frey, 1984). Purification and separation of monomeric forms from aggregates and the synthesis of dimeric clusters were described by Yang and Frey (1984). The methods of suspending gc 21+ in sodium chloride solutions and the desalting for experimental purposes were presented by Reardon and Frey (1984), by Yang and Frey (1984), and by Eskelinen and Peura (1988). Undecagold clusters with no electrostatic charges and undecagold clusters with negative electrostatic charges were prepared according to Reardon and Frey (1984).

Cationized ferritin was obtained from commercial sources both from Miles Laboratories, Indiana, and from Sigma, St. Louis, prepared by the method of Danon *et al.* (1972) and suspended in saline. One vial contained some undetermined amount of ionized iron which induces inhibition of mitochondrial respiration, as is observed with commercial ferritin from several sources.

Preparation of organelles and macromolecules

Heart mitochondria were obtained by differential centrifugation of beef heart homogenates by the methods described by Crane *et al.* (1956) which also separated a lighter population of light beef heart mitochondria (LBHM) from well-coupled heavy beef heart mitochondria (HBHM).

The functional differences between coupled and uncoupled mitochondria were described by Chance and Williams (1956) when they described mitochondrial respiratory control in state 3, in the presence of ADP, and by Hunter *et al.* (1976) in the presence of uncouplers. Preparations of HBHM were well-coupled when they had high respiratory control, or had high stimulation of respiration in the presence of uncouplers as seen in the presence of DNP in Figure 2 and in Table 1. LBHM had low respiratory control and responded poorly to the presence of uncouplers. Fragments of inner mitochondria membranes were prepared according to Löw and Vallin (1963) in the medium described by Hansen and Smith (1964), and coded as electron transport particles from the heart (ETPH). The concentration of mitochondria and particles was measured by determining protein content by the method of Gornall *et al.* (1949). Methods to evaluate oxidative phosphorylation coupling were described by Hansen and Smith (1964), Chance and Williams (1956) and Hatefi (1985).

1 Synthesis of the Undecagold Cluster

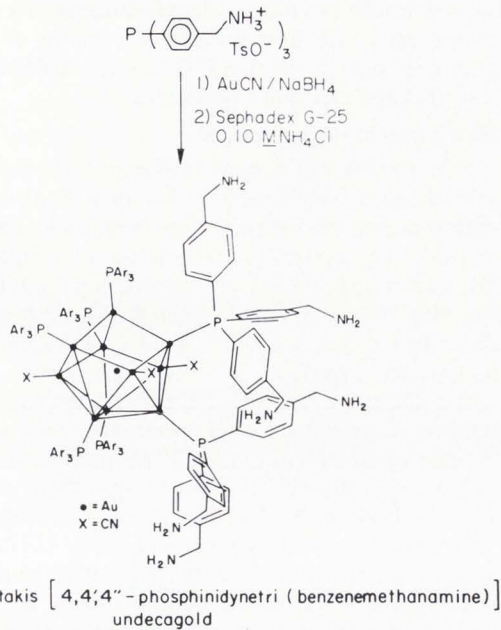


Figure 1. Synthesis and structure of the undecagold cluster (gc 21+).

Table 1: Effects of artificial electron dense probes on mitochondrial respiration during succinate oxidation. Oxygen uptake is measured with a Beckman teflon membrane oxygen electrode in a thermostated closed double vessel. The inhibition of LBHM by gc 21+ and by cationized ferritin varies but in one minute reaches to no oxygen uptake.

_____ nanoatoms of oxygen uptake
mitochondrial mg of protein x minute

Heavy beef heart mitochondria (HBHM)

No additions	30.5 ± 1.6	(n = 89)
gc ²¹⁺ (2 μM)	51.9 ± 2.8	(n = 20)
gc ⁰ charges (10 μM)	30.2 ± 2.1	(n = 6)
gc ⁽⁻⁾ (10 μM)	30.2 ± 2.4	(n = 14)
Cationic ferritin (2 nM or 1.2 mg of protein)	64.7 ± 6.2	(n = 14)
A23187 (2 nM)	73.2 ± 3.7	(n = 12)
DNP (10 μM)	72.2 ± 5.3	(n = 15)

Light beef heart mitochondria (LBHM)

No additions	84 ± 8.7	(n = 18)
DNP (10 μM)	86 ± 6.7	(n = 20)
A23187 (2 nM)	85 ± 7.2	(n = 10)
gc ²¹⁺ (2 μM)	0	(n = 16)
Cationic ferritin (2 nM or 1.2 mg of protein)	0	(n = 12)

2

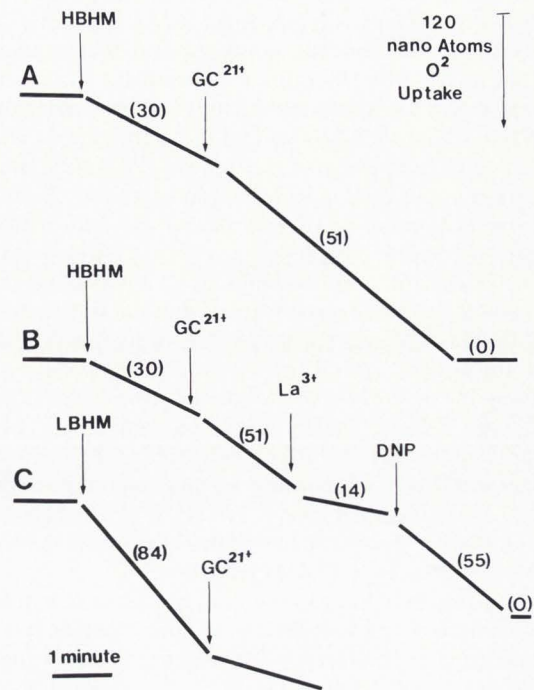


Figure 2. Changes in mitochondrial respiratory rates induced by 0.5 M cationic gold cluster (gc 21+) per mg. of mitochondrial protein. A. Oxygen uptake trace shows gc 21+ stimulation of well-coupled heavy beef heart mitochondria (HBHM) respiration using 5 mM succinate as substrate. B. The experiments show that La (10 nanoM of Lanthanum chloride) inhibits the gc 21+ stimulation of well-coupled HBHM respiration using succinate as substrate. This inhibition is released by 50 μM of dinitrophenol (DNP). C. This record of oxygen uptake demonstrates that succinate oxidation by light beef heart mitochondria (LBHM) is inhibited by gc 21+. Numbers in parentheses are the rates of oxygen uptake in nanoatoms of oxygen consumed per mg of protein per minute. pH of medium is maintained at 7.4 using Tris buffer HCl.

Preparation of *E. coli* pyruvate dehydrogenase and its components E1, E2 and E3 were described by CaJacob *et al.* (1985). The preparation of pyruvate dehydrogenase had a specific activity of 48 units/mg of protein. It was stored at -70 °C and when used diluted in 0.1M Tris buffer because gc 21+ aggregates in the presence of phosphate buffer, probably a phosphate effect. Glutamate dehydrogenase was purified from beef liver mitochondria by the procedure of Fahien *et al.* (1969). Membranous cytochrome oxidase particles was prepared according to Sun *et al.* (1968).

Electron microscopy procedures

Samples of the suspended and sometimes respiring organelles, or their fractions, were fixed by adding 4% glutaraldehyde in 0.2 M cacodylate buffer to the test medium to reach a final concentration of 2% glutaralde-

hyde and 0.1 M cacodylate buffer. The fixative was added in sufficient volumes to adjust to the proper concentration. Fixation was continued at 5 °C temperature for one hour. After fixation, the specimens were washed repeatedly in 0.1 M cacodylate buffer. Optional staining and fixation were added with 1% osmic acid in 0.1 M collidine buffer, and in some groups 2% uranyl acetate was used in the 25% dehydrant ethyl alcohol. Dehydration was accomplished in successively more concentrated grades of ethanol, dry propylene oxide, propylene oxide-resin series, and resin embedding in equal mixtures of Epon-Araldite. The possibility of thermal destruction of the undecagold clusters at 58 °C, which was usually used for polymerizing Epon-Araldite, suggested the embedding in LR White resin (obtained from Ernest Fullam Inc., 900 Albany Shaker Road, Latham, NY, 12110). To prevent heat of polymerization, these specimens were processed at 4 °C according to manufacturers instructions. Unstained and uranyl acetate-lead citrate stained sections are cut with diamond knives for transmission electron microscopy (TEM) examination.

Grids for TEM examination were also prepared by depositing unfixed suspensions of specimens on butyvar coated grids. Fixed suspensions required carbon coating and wetting with 1% bacitracin. These suspensions contained approximately 1 mg of protein per ml. Excess fluid was absorbed with filter paper and in most cases room temperature drying was obtained in open air. Liquid nitrogen freezing and freeze-drying, critical-point method, and negative staining by the method of Brenner and Horne (1959) with phosphotungstic acid were used to prepare grids. Additional technical information for these procedures was described by Gregory and Pirie (1973), Pease (1964), Munn (1968), and Muscatello and Horne (1968) for the use of PTA and the value of isoosmotic ammonium molybdate for negative staining of unfixed specimens.

TEM was performed with a Hitachi 11E, a JEOL 100 CX, and the AEI EM7 million volt instrument. The bright field mode was used routinely. Dark field techniques were used following manufacturers instructions. The million volt instrument had hollow cone illumination for dark field. The JEOL 100 CX used beam tilting and objective aperture adjustments.

The energy dispersive X-ray analysis was done in a JEOL 100 CX instrument using 100 kV and the scanning transmission mode, detection of elements was obtained with a Kevex detector and appropriate computer system. The detection of gold was straight forward but the sensitivity was low because in the available instrument, a JEOL 100 CX, the detector-target difference was set for metal materials. Magnification of 20,000X and scanned areas showed the presence of gold atoms in areas which were 20% of the area visualized in a section of a control HBHM which was approximately one μm^2 . The areas measured in our experiments with the JEOL 100 CX instrument averaged 20×10^6 square Ångströms. Similar measurements and detection of gold in sections of isolated mitochondria were obtained at 100 kV with

a JEOL 200 CX and Tracor Northern detector and computer. The areas analyzed, in a rastered area or spot, were estimated to measure approximately 1×10^6 square Ångströms. Smaller areas, by a factor of 5X, were obtained with a Vacuum Generator HB500 scanning transmission electron microscope.

Biochemical measurements

The rates of oxygen consumption by isolated heart mitochondria were measured with a Beckman oxygen electrode which had a teflon membrane covering the sensor. The system had regulation of temperature and allowed measurements of protons, potassium and calcium ions, separately or in tandem. These methods were described by Rzeczycki and Valdivia (1973) and Blondin and Green (1969).

Calcium content of the mitochondria was measured by atomic absorption spectroscopy by methods described by Reed and Lardy (1972) and by Murthy *et al.* (1973). Kinetic effects induced by A23187, Lanthanum (La), Strontium, EGTA, EDTA, on respiring mitochondria were described by Reed and Lardy (1972) and provided evidence of calcium fluxes in mitochondrial respiring systems. A23187 is believed to be an ionophore, and in these experiments activator of calcium efflux; La is an inhibitor of calcium influx; strontium was also an inhibitor of calcium influx; EGTA and EDTA are calcium chelators and prevent the calcium cycling started by release with A23187 (Reed and Lardy, 1972). The apparatus used for incubation and measurements of fluxes was made of a double walled glass vessel which had water circulation and temperature regulation. The inside of the vessel had a closed capacity of 10 ml or less and a pore for injection of reagents. Media used were isoosmolar sucrose, or KCl, with additional substrate, usually succinate 5 mM. The pH of the medium was maintained at 7.4 with tris HCl buffer. The calcium fluxes were detected with commercial electrodes, Beckman and Orion. Determination of calcium content of mitochondria was obtained by addition of the suspended organelles into heavy walled polypropylene tubes and pelleted in a high speed centrifuge with sedimentation completed in approximately 30 seconds. The suspension solution was decanted, the tubes inside wiped dry and the pellets were lysed in deionized water and subsequently extracted with 0.1 perchloric acid [for calcium, magnesium or inorganic phosphate] or 0.1 N HCl for potassium. Calcium, magnesium and potassium were measured with Perkin Elmers 303 or 403 atomic absorption spectrophotometers. Strontium chloride was included in all samples at one per cent to prevent interference with phosphate.

Measurements of gc 21+ binding

The concentration of gc 21+ was measured by spectrophotometry in a Gary 500 and a Hitachi double beam spectrophotometer at 415 nanometers wave length using an extinction coefficient of $2.95 \times 10^4 \text{ M}^{-1} \text{ cm}^{-1}$ (Reardon and Frey, 1984). Standard curves at different concentrations of gc 21+ were obtained using saline,

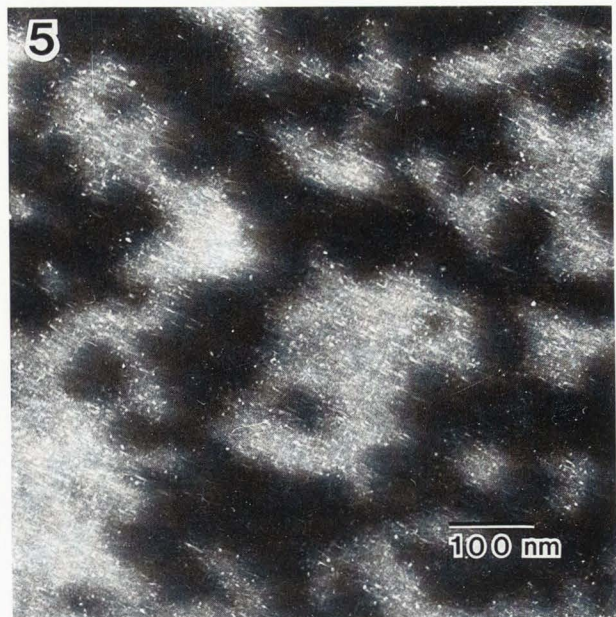
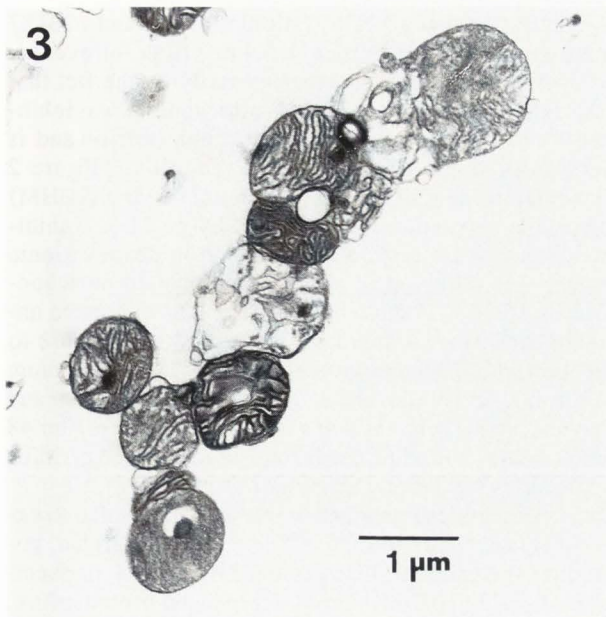


Figure 3. Population of heavy beef heart mitochondria are exposed to gc 21+. The mitochondria are clumped. Respiring HBHM are fixed in glutaraldehyde one minute after gc 21+ addition (see Fig. 2). Glutaraldehyde fixation is followed by osmium, embedding, sectioning and staining with uranyl acetate-lead citrate. TEM. Bright field. Some mitochondria develop an orthodox (or expanded) transition (Hunter *et al.*, 1976).

Figure 4. Light beef heart mitochondria (LBHM) are respiring succinate and are exposed to gc 21+. The fused membranes form rolls which simulate myelin structure. X-ray microanalysis demonstrates presence of gold in these structures. Glutaraldehyde fixation is followed by osmium, sectioned and stained with uranyl acetate-lead citrate.

Figure 5. Pyruvate dehydrogenase bound to gc 21+. Pyruvate dehydrogenase complexes have been exposed to gc 21+ and then fixed in 0.5% glutaraldehyde, washed and suspended particles are deposited on carbon films supported on formvar coated grids. These preparations are stained with 2% neutral phosphotungstic acid and studied by dark field TEM. The white structures are aggregated enzyme complexes, the small bright structures are believed to be gc 21+. Dark field TEM, JEOL 100 CX.

and mediums used for binding and functional studies. Measurements were obtained by withdrawal of gc 21+ containing medium and test organelles or enzymatic complexes using a syringe and a Millipore filter 0.2 μm pore size. Additional centrifugation to separate the gc 21+ containing medium from the test system was done with an Eppendorff centrifuge (10,000 gs) or Beckman L275 ultracentrifuge (30,000 gs). Gc 21+ measurements were made in supernatants after appropriate centrifugation in medium at different times, before and after fixation.

Results

Binding of undecagold cluster

The binding of gc 21+ to isolated mitochondria, pyruvate dehydrogenase and glutamate dehydrogenase occurred rapidly at concentrations of 2 mg protein reacting with 1 μM of gc 21+. The experiments were performed in the cuvette and apparatus described above in methods to measure oxygen consumption and ionic fluxes. Respiring heavy beef heart mitochondria (HBHM), 2 mg protein per ml of medium were exposed

to 1 μM gc 21+ and 50% binding was observed at the end of one minute and almost 100% at the end of three minutes. The effects of gc 21+ on isolated respiring mitochondria were observed within 10 seconds (see Figure 2). Mitochondria and enzymatic systems were observed to clump and precipitate rapidly within three minutes after exposure to gc 21+. Electron microscopy showed clumping of the particles (Figs. 3, 4 and 5). Observations and measurements of gc 21+ binding to light beef heart mitochondria showed similar organelle clumping but binding is 70% at the end of three minutes of exposure to the gc 21+.

Influence of gc 21+ on mitochondria respiration and ionic fluxes

Gc 21+ accelerated respiration of heavy beef heart mitochondria (HBHM) in a modified state 4 (Fig. 2 and Table 1). We refer our results to be in a modified state 4 of Chance and Williams because we used tris HCl buffer while Chance and Williams (1956) state 4 used phosphate buffer. The experiments with gc 21+ depicted in Fig. 2 and Table 1 showed increased oxygen uptake in the absence of added calcium, phosphate or ADP. In experiments with phosphate and ADP, the respiratory control index of HBHM was greater than 4. The gc 21+ induced increase of oxygen uptake was inhibited by LaCl_3 , a competitive inhibitor of calcium uptake as demonstrated by Reed and Lardy (1972). EDTA, LaCl_3 and EGTA depressed gc 21+ accelerated mitochondrial respiration probably by EDTA and EGTA complexing ionizable calcium present in the medium or by inhibiting calcium uptake by the calcium carrier as postulated by Reed and Lardy (1972). Simultaneous measurements of oxygen and pH with calibrated electrodes showed that gc 21+ induced both an increase of oxygen consumption and a simultaneous increase in the pH of the medium. Reed and Lardy (1972) have reported similar experimental results using isolated rat liver mitochondria exposed to A23187 and they have proposed that the ionophore induces calcium release followed by calcium cycling. Exposure of HBHM to A23187 resulted in acceleration of respiration (see Table 1) which was also inhibited by La, EDTA and EGTA. Chemically derivatized gc which retained the positive charges, e.g., dimethylated amino groups, exhibited behavior similar to gc 21+, while gc with peripheral negative electrostatic charges, e.g., succinylated gc, or clusters with zwitterionic peripheral groups resulting from carboxymethylation of the amino groups exhibited no effects on succinate respiring mitochondria (see Table 1) and no binding was detected.

Support for the hypothesis that nonpenetrating cationic probes induce calcium fluxes and accelerate succinate respiration of HBHM was provided by experiments using cationic ferritin prepared by coupling horse spleen ferritin via carbodiimide activation of the majority of available carboxyl groups which showed a similar increase in oxygen uptake and inhibition by La, EDTA and EGTA. Furthermore, cationic ferritin was clearly visualized by TEM as being only on the outer mitochondrial membrane (Figure 6). Additional support for the

interpretation that gc 21+, cationic ferritin and A23187 independently induce HBHM calcium efflux followed by its cycling was provided experimentally by the fact that respiration of calcium depleted mitochondria was inhibited by exposure to gc 21+ and cationic ferritin and is not modified by A23187 or DNP addition. Figure 2 demonstrates that light beef heart mitochondria (LBHM) succinate respiration was inhibited by gc 21+. Inhibition of succinate respiration by electron dense cationic probes was observed in all calcium depleted mitochondria, in LBHM, in mitochondria which have become unstable because of preparative techniques or exposure to medium which induces spontaneous discharge of calcium according to Hunter *et al.* (1976), after freezing and thawing, in mitochondria exposed to uncouplers, after 48 hours aging, and after conditions which induce pyridine nucleotides oxidation (Lehninger *et al.*, 1978).

Electrodes immersed in test medium similar to experiments depicted in Figure 2 demonstrated proton, potassium and calcium fluxes induced by gc 21+ on succinate respiring HBHM. Gc 21+ produced proton influx, potassium and calcium effluxes. Replacement of sucrose Tris medium for 150 mM potassium chloride buffered to pH 7.4 with Tris produces similar results to experiments in Figure 2. Similar results are also obtained with glutamate, malate, ketoglutarate, pyruvate and hydroxybutyrate substrates.

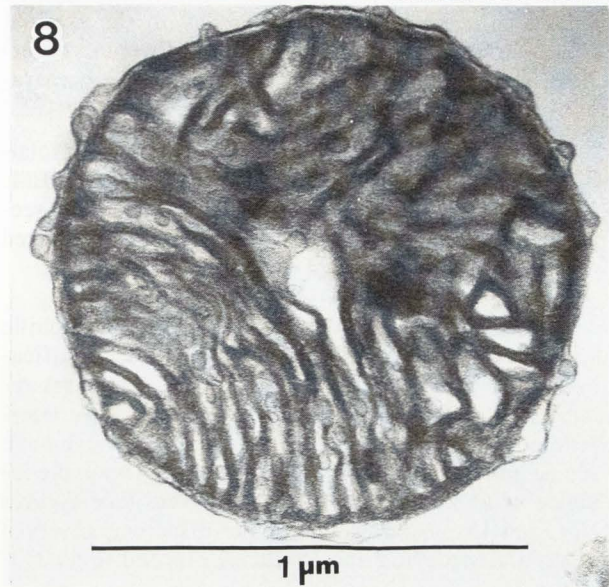
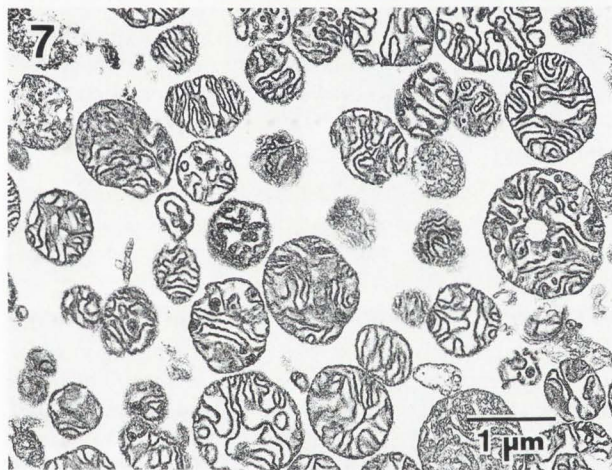
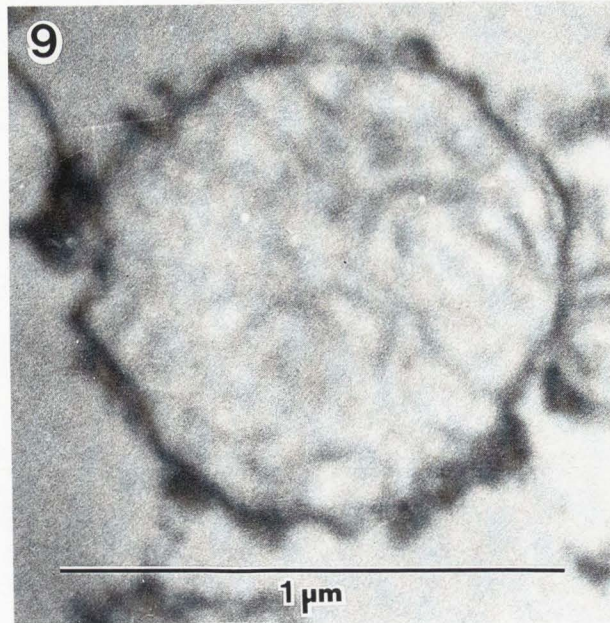
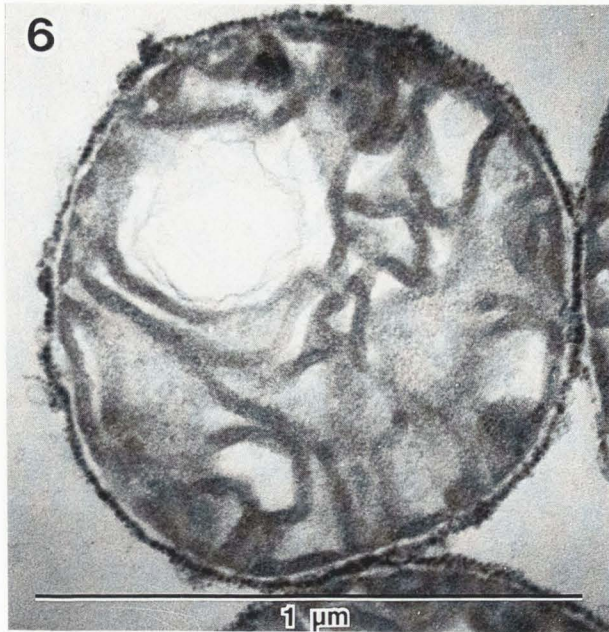
Calcium fluxes

The experiments using the appropriate electrodes demonstrated that HBHM released calcium after addition of gc 21+ since HBHM have 30 nanomoles of calcium per mg of mitochondrial protein and when measured after gc 21+ exposure they are found to contain around 18 nanomoles of calcium, which is the appropriate content of DNP exposed HBHM and of LBHM.

Morphologic observations of the effects of undecagold clusters binding to respiring heavy beef heart mitochondria

The classic description of mitochondria in cells by Palade (1952) required the development of fixation, embedding, sectioning and advances in the instrumentation of TEM. A review of mitochondrial morphology compartments and membranes is found in books by Munn (1974) and Tandler and Hoppel (1972). Control, isolated heavy beef heart mitochondria are presented in Figure 7 with a representative population at low magnification. One, HBHM, is depicted in Figure 8. Isolated HBHM are apparently spherical and have a collapsed matrix space when fixed during respiration with succinate as substrate and conditions and medium described in Figure 2. Sumegi *et al.* (1988) have described compartments and membrane dominions which separate outer and inner membranes as well as links between the membranes.

Thin sections of resin embedded pellets of isolated heavy beef heart mitochondria exposed to gc 21+ fixed with glutaraldehyde, showed electron dense material on the outside of the organelles (see Figure 9); the



Figures 6-9: Bright Field. TEM.

Figure 6. Single isolated heavy beef heart mitochondria (HBHM) is exposed to cationized ferritin during respiration with succinate (see Fig. 2). Mitochondria are fixed in glutaraldehyde followed by osmic acid and are sectioned and stained with uranyl acetate-lead citrate. The particles of cationized ferritin are seen on the external surface of the outer mitochondrial membrane.

Figure 7. Population of isolated heavy beef heart (HBHM) respiring with succinate as substrate (see Fig. 2), fixed in glutaraldehyde followed by osmic acid. Embedding is in Epon-Araldite resin and sectioned. Staining is with uranyl acetate-lead citrate.

Figure 8. Single heavy beef heart mitochondria (HBHM). Staining is with uranyl acetate-lead citrate.

Figure 9. Single isolated heavy beef heart mitochondria (HBHM) exposed to gc 21+ during respiration with succinate (see Fig. 2), fixed in glutaraldehyde, no osmic acid exposure and no staining. Electron opaque material is observed on the outside of the mitochondria.

electron dense material developed higher electron density after osmic acid exposure (osmiophilia), see Figures 4 and 10. Lead and uranyl staining enhanced the effects of osmium treatment.

The sections of light beef heart mitochondria exposed to gc 21+ which induce a rapid inhibition of succinate respiration (see Figure 2) have a predominance of swollen inner membrane matrix and distinct granular material on the external surface which have electron dense osmiophilic minute spheres which may represent the osmium stained gc 21+. An electron micrograph of a section of control LBHM is presented in Figure 11. Our examinations suggest that thin sectioning and tangential cuts of membranes may facilitate localization of the labels (Figures 12 and 13).

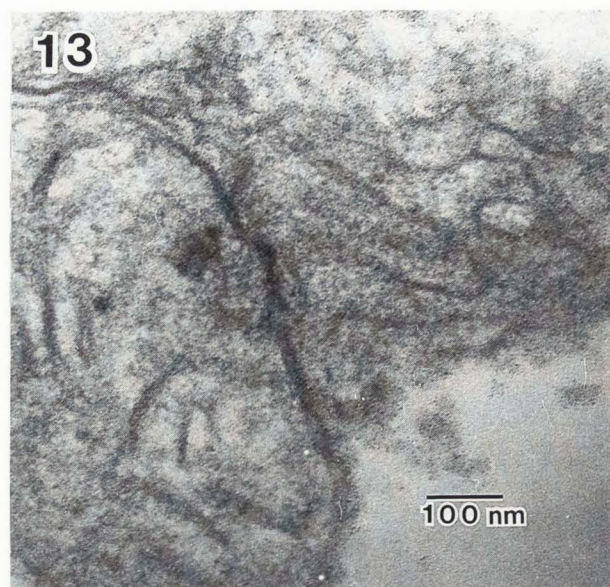
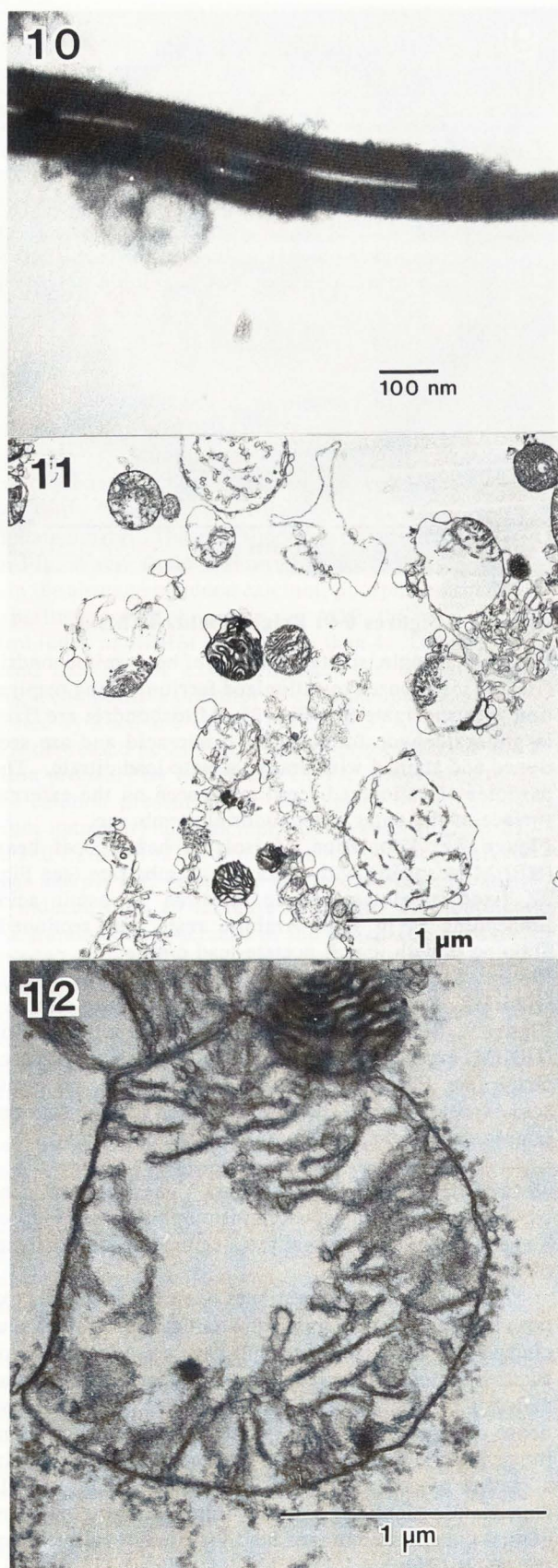


Figure 10. Lamellar cytochrome oxidase exposed to gc 21+. Sections are stained with uranyl acetate-lead citrate. Bright field shows thicker fused membranes with distinct osmiophilic material observed between the membranes.

Figure 11. Population of isolated light beef heart mitochondria (LBHM) fixed in glutaraldehyde followed by osmium, sections stained with uranyl acetate-lead citrate. Bright field. TEM

Figure 12. Isolated light beef heart mitochondria (LBHM) are exposed to gc 21+ while respiring in succinate. The mitochondria are fixed in glutaraldehyde one minute after gc 21+ addition followed by osmic acid. The resin blocks are thin sectioned and stained in uranyl acetate-lead citrate. Bright field. TEM. Osmiophilic granular material is observed adherent to the external surface of the outer mitochondrial membrane; this observation is not demonstrated in respiring HBHM preparations exposed to gc 21+ for up to 3 minutes.

Figure 13. Isolated LBHM exposed to gc 21+. Isolated LBHM treated like in Figure 12. Bright field. TEM. Small granular osmiophilic material on a tangential section of the outer mitochondrial membrane is interpreted to represent osmium stained gc 21+.

Some of the LBHM sections showed osmiophilic electron dense structures which at high TEM magnifications had concentric repeating membrane structures resembling the ultrastructure of nerve myelin. We interpret these structures to be fused membranes which have become adherent to each other, presumably upon the influence of gc 21+ to the binding surfaces (see Figures 4, 14, and 15). Similar membrane fusion was observed in membranous cytochrome oxidase exposed to gc 21+ (Figure 10).

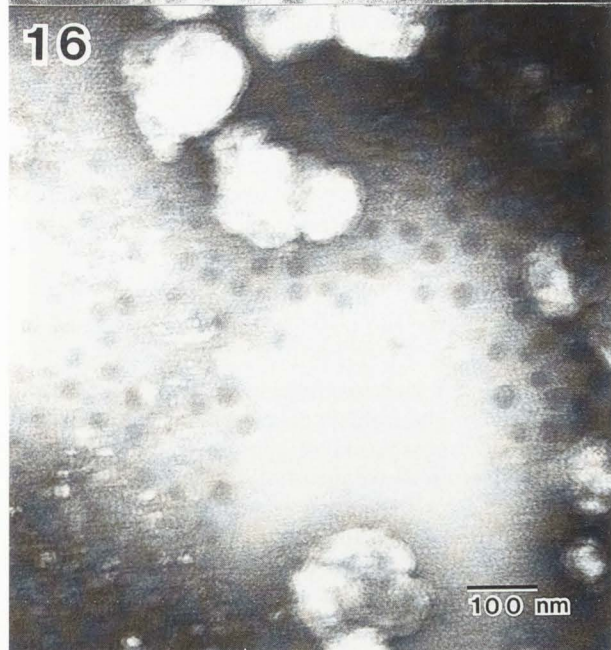
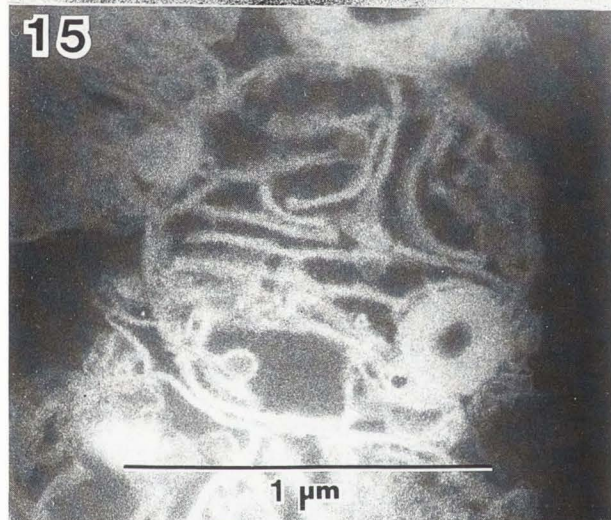
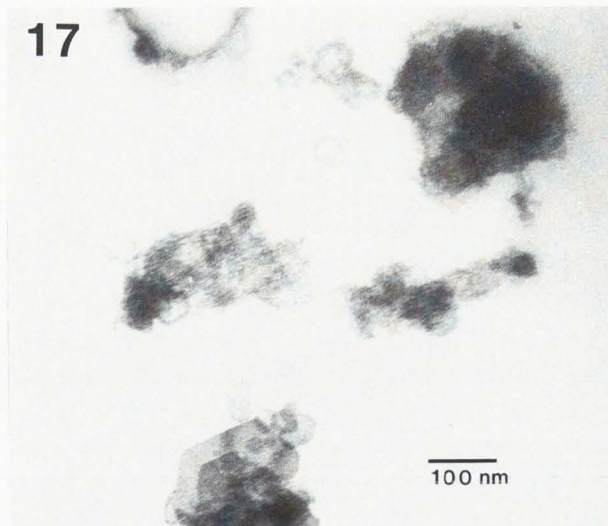
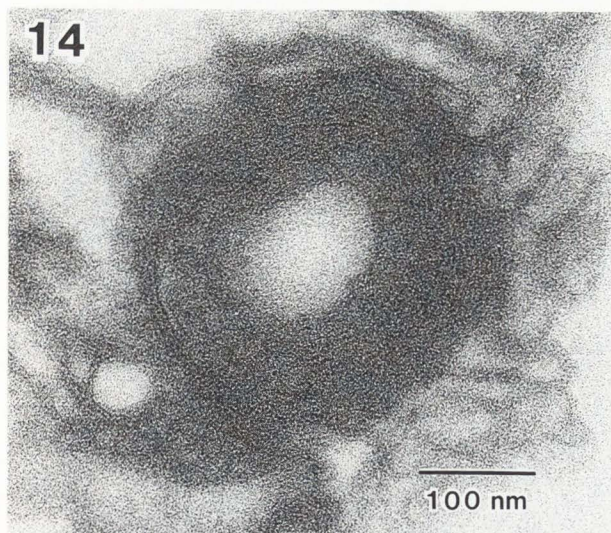


Figure 14. Light beef heart mitochondria (LBHM) same as Fig. 4. Fused membranes form concentric rings or rolls.

Figure 15. Isolated light beef heart mitochondria (LBHM) exposed to gc 21+ (see Fig. 1) are fixed in glutaraldehyde followed by osmium. The resin blocks are thin sectioned and stained with uranyl acetate-lead citrate. Dark field. JEOL 100 CX TEM. Membranes are more distinct and gold is found by energy-dispersive X-ray microanalysis using JEOL 100 CX and JEOL 200 CS instruments in the circular structures.

Figure 16. Electron transport particles, heart (ETPH) are exposed to gc 21+. A suspension of ETPH, 1 mg protein in 1 ml of Hansen preserving medium (Hansen and Smith, 1964) is mixed with gc 21+ to make a solution of 5 μ M gc 21+. The particles exposed to gc 21+ are deposited on carbon coated, formvar covered grids; excess fluid is removed with filter paper and the dry preparation examined by dark field TEM in a JEOL 100 CX instrument. Patches of bright areas are seen in the vesicular structures and are interpreted to be gc 21+ material. The electron micrograph demonstrates some drift of the specimen because of the presence of gold.

Figure 17. Vesicular cytochrome oxidase prepared according to Sun *et al.* (1968) has been diluted with sucrose-tris to a concentration of 1 mg protein per ml and then mixed with 50 μ l of gc 21 for a concentration of gold of 10 μ M. After 5 minutes of incubation, the specimens have been fixed in 2% glutaraldehyde followed by osmic acid, dehydration and embedding in resin; see methods. Thin sections are stained with uranyl acetate-lead citrate and examined with bright field TEM. The vesicles are aggregated, osmiophilic material is seen in patches outside the vesicles, electron dense material is seen in nonvesicular aggregates and few crystals are observed.

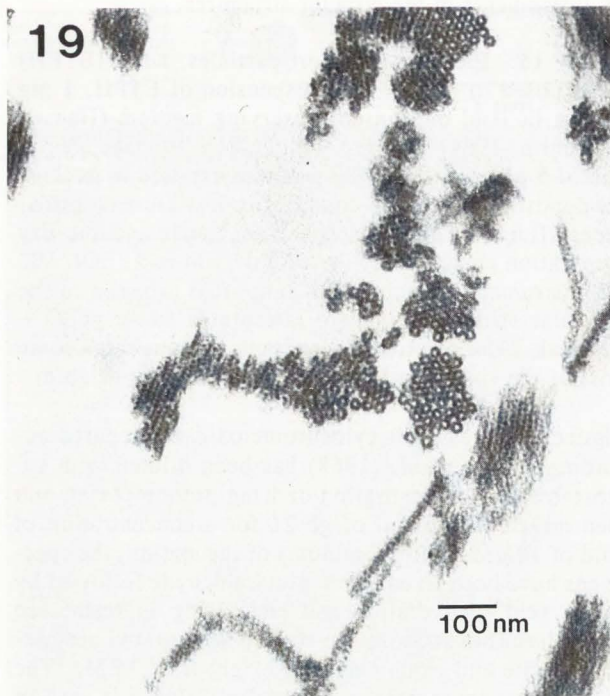
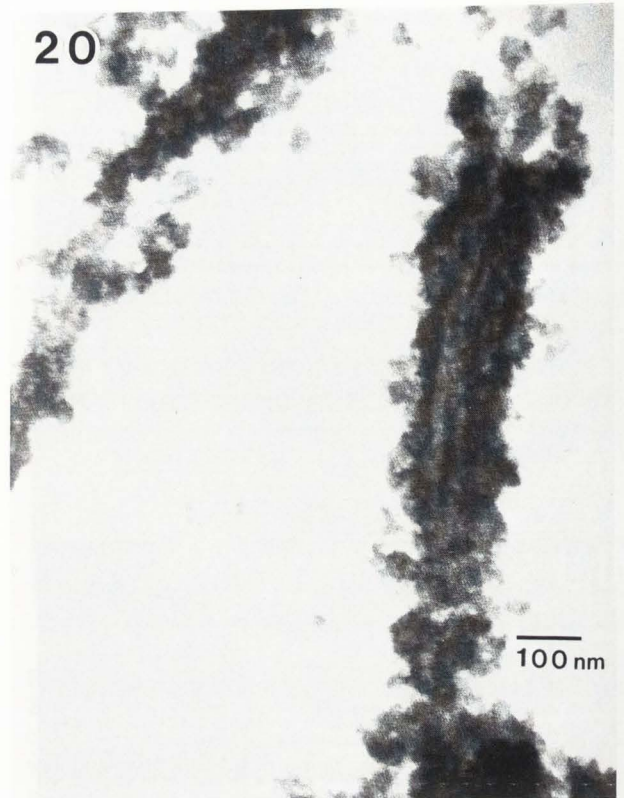


Figure 18. Lamellar cytochrome oxidase. Control sections prepared as Figure 17.

Figure 19. Crystallized glutamate dehydrogenase isolated from beef liver. The enzyme has been fixed in 2% glutaraldehyde and resin embedded. Thin sections are stained with uranyl acetate-lead citrate as described in the text. The photograph shows cross-sections of tubes, oblique and some longitudinal sections of the tubes.

Figure 20. Crystallized glutamate dehydrogenase isolated from beef liver and exposed to gc 21+. These sections demonstrate obliteration of the tubular structures and osmiophilic material outside and in the walls of the tubular structures.

Morphology of electron transport particles exposed to gc 21+

Sections of electron transport particles of heart (ETPH) fixed in glutaraldehyde and embedded in Epon-Araldite show aggregation of the ETPH and distinct patches of electron dense material on the outside of the aggregated vesicles. The dense material was osmiophilic and stains more with lead citrate. Negatively stained material and material examined without staining demonstrated vesicles with patches of electron dense material that showed some drifting when exposed to the electron beam (Figure 16).

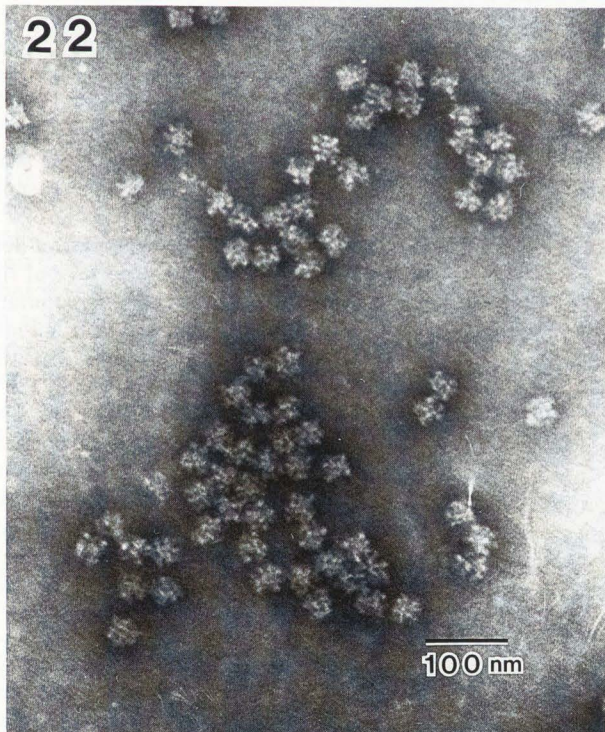
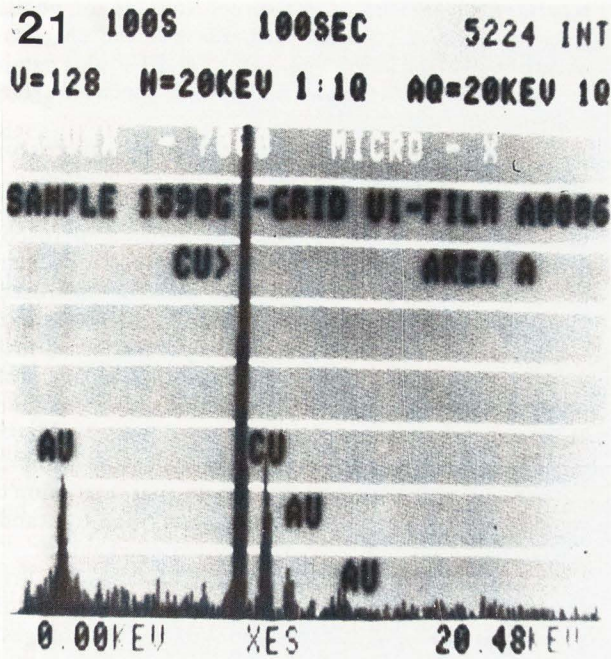


Figure 21. X-ray spectrum showing gold signal.
Figure 22. Negatively stained isolated bacterial pyruvate dehydrogenase. The enzyme complexes are fixed in 0.5% glutaraldehyde and after washing out the fixative, the particles are deposited on carbon films supported on formvar coated grids. These preparations are stained with 2% neutral phosphotungstic acid and photographed in bright field TEM.

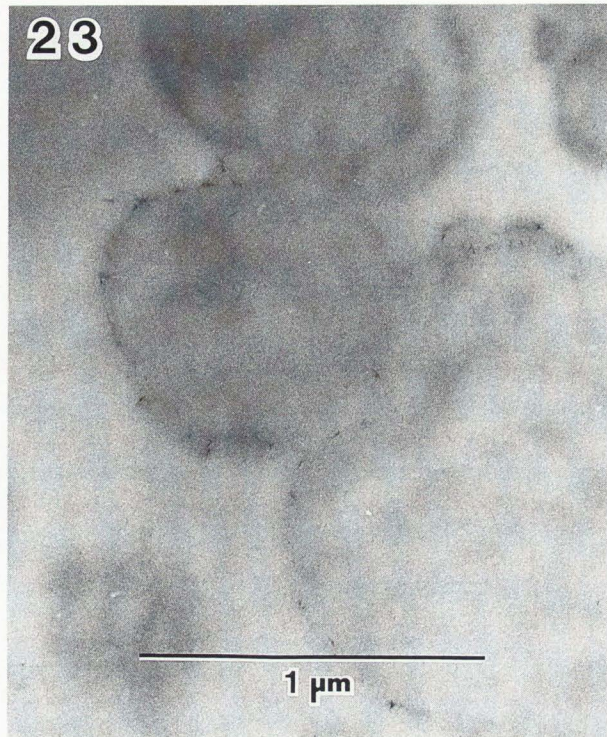


Figure 23. HBHM exposed to gc 21+ and La^{3+} . Isolated heavy been heart mitochondria are respiring in succinate and are exposed sequentially to gc 21+ and $LaCl_3$. Mitochondria are fixed in glutaraldehyde, embedded in LR White resin, thin sectioned and observed in bright field mode TEM. Small electron dense thin needle-like particles on the outer mitochondrial membrane are interpreted to be $LaCl_3$. Smaller, less electron dense gc 21+ are not apparent without osmium staining.

Membranous cytochrome oxidase

The suspension of membranous cytochrome oxidase is composed of vesicles and membranous lamellae. Gc 21+ aggregated the vesicles and adhered to their external surface (Figure 17). Sections of lamellae apparently developed thicker single membranes (Figures 10 and 18) than the control but the intermembrane measurement in both cases is 8.3 nm. The gc 21+ bound cytochrome oxidase lamellae had more dark stained material between the nonstained membranes probably due to the presence of the osmiophilic gc 21+ probes.

Glutamate dehydrogenase

Beef liver glutamate dehydrogenase crystallizes readily (Fahien *et al.* 1969). Filamentous and tubular structures were observed with the light and electron microscopes. The diameter of the glutamate dehydrogenase tubes in negatively stained preparations is approximately 20 nm. The uranyl acetate-lead citrate stained thin sections of resin embedded crystallized enzyme demonstrated a tube diameter of 18 nm (Figure 19).

Bright field TEM showed that gc 21+ binds to the glutamate dehydrogenase tubules (Figure 20). Obliteration of their tubular structure demonstrated that gc 21+ binding induced changes of the enzyme ultrastructure.

Energy dispersive X-ray analysis

Samples of mitochondria bound to gc 21+ have been examined by JEOL USA Inc. with a JEOL 200 CX instrument and at the College of Engineering (Material Sciences Laboratory, Mr. R.J. Casper), with a JEOL 200 CX instrument. These studies showed strong gold signals in the mitochondria (Figure 21) but indistinct location except in the LBHM area of membrane fusion which definitely show the presence of gold labelled membranes.

Dark field transmission electron microscopy

Dark field electron microscopy of coated grids with unstained specimens, negatively stained and resin embedded sections have been examined with the AEI EM7 million volt electron microscope, Hitachi 11E and JEOL 100 CX microscopes with beam tilt and/or objective aperture displacement techniques as directed by the instruments manuals. A combination of electron beam tilt and objective aperture adjustments provided comparative better resolution. Control electron micrographs of isolated pyruvate dehydrogenase, negatively stained, were visualized in Figure 22. Visualization of the gc 21+ electron probes was distinct in the preparation of unstained pyruvate dehydrogenase (Fig. 5). Unstained and osmic acid stained sections show bright membrane structures in the periphery of LBHM, in the myelin-like membrane roll images and in the outside of HBHM.

The million volt microscope had the facilities for hollow cone illumination for dark field but the results obtained have similar resolution when compared to dark field observations with beam tilting and objective aperture adjustments with the JEOL 100 CX instrument.

Visualization of electron dense probes by electron microscopy

Availability of transmission electron microscopes capable of providing high resolutions in the Ångström dimensions suggested that visualization of 1 nm electron dense probes may be feasible under proper experimental conditions. The visualization of undecagold cluster was possible with TEM in bright field mode dependent on the designing of the specimen preparation, sectioning, fixation and localization since the 0.8 to 1 nm size requires minimum overlapping of structures. Micrographs with the JEOL 100 CX microscope and the AEI EM7 million volt modified microscope of the Wisconsin High Voltage Facility allowed visualization of electron dense membranes with increased electron densities due to gc 21+ binding (see Fig. 9). Specimen preparation, particular experimental design, and appropriate electron microscopy instrumentation are absolute requirements for individual visualization of these small probes (Hainfeld, 1987; Safer *et al.*, 1986; Kuhn *et al.*, 1984; Lipka *et al.*, 1983; Wall *et al.*, 1982; Wall, 1978). Qualitative comparison of micrographs of osmicated and non-osmicated specimens showed that gc 21+ clusters were osmiophilic. These

results were confirmed by direct staining of gc 21+ suspensions with osmium tetroxide and the changes in absorbance of gc 21+ compared to gc 21+ plus osmium tetroxide in the ultraviolet and visible spectrum (results not shown).

The changes observed by electron microscopic studies of the mitochondria, glutamate dehydrogenase, membranous ETPH and of membranous cytochrome oxidase suggested that gc 21+ binding induced microscopic alterations of the ultrastructure of these macromolecular systems. The simulation of the electron microscope structure of nerve myelin by three separate membranous systems bound to gc 21+ suggests that membrane fusion may occur and explains the lamellar formation and probably three-dimensional crystallization of membranous structures as demonstrated in purple membranes by Henderson and Smith (1980). Differences in membrane appearance may be secondary to molecular dimension differences, changes in hydration as described by Rand *et al.* (1979) in myelin or by some other mechanism.

Examination of micrographs obtained by bright field electron microscopy of Epon-Araldite embedding sections at final magnifications above 150,000X suggested that approximately 1 nm particles were present on the outside of the outer mitochondrial membranes. Our observations suggested that the gc 21+ binding may occur in patches that may be due to dehydration of the organelles secondary to processing. These particles were osmiophilic and appeared to stain more distinctly with lead citrate. This is a subjective description which has ruled out stain precipitation secondary to electron exposure which has not been observed in any of the electron microscopes used.

Apparent visualization of the small electron dense probes, gc 21+, was more distinct on the surface of light beef heart mitochondria because this organelle population presents projections on the outer surface of swollen mitochondria (see Figure 12) and had more tangential sections of membranes such as presented in Figure 13.

Examination of LR White embedded sections processed and stained as the Epon-Araldite embedded material presented similar electron dense particles that we interpret to represent gc 21+. The minute size of the probe is also enhanced by osmium and staining. Mitochondria exposed to gc 21+ and lanthanum (see Figure 23) demonstrate small electron dense needles 10 to 20 nm long which are more electron dense than the smaller gc 21+ particles. We believe that these small needle-like structures represent lanthanum. We were unable to distinguish between the ultrastructure of organelles embedded in LR White and Epon-Araldite, respectively.

Discussion

We have investigated functional and morphological alterations induced by binding of undecagold clusters to respiring isolated heart mitochondria and to other macromolecular systems. These studies encompass the following: first, electrostatic dependent binding of mitochondria to undecagold clusters; second, respiratory changes in-

duced by the binding of gc 21+ to mitochondria; and third, morphologic alterations induced on isolated mitochondria and macromolecules by exposure and binding to undecagold clusters.

Undecagold binding to isolated heart mitochondria

Our experiments demonstrate that biologic systems which have electrostatic negative charges (mitochondria, pyruvate dehydrogenase, glutamate dehydrogenase) and are known to have outside surface negative charges, bind avidly to positively charged artificial electron dense probes. The experiments with cationized ferritin clearly confirm that the mitochondrial binding of the electron probes is on the outside of the outer mitochondrial membrane of HBHM. These experiments suggest that under these test conditions both cationized ferritin and gc 21+ induce functional and morphologic changes without penetration of the probes beyond the outer surface of the exposed membranes. In respiring HBHM the probes are seen covering the surface of the outer mitochondrial membrane. Under similar experimental situations, positively charged probes must bind to the outer surface of the cell membrane because eukaryotic cells and mitochondria have a net negative charge which is demonstrated by electrophoresis experiments (Valdivia *et al.*, 1973). Alternative explanations to the gc 21+ binding to respiring HBHM under the test conditions described for Figure 2, curve A, are that the net negative charge of respiring mitochondria requires additional factors to explain the rapid gc 21+ binding to the outside of the outer mitochondrial membrane and the induction of the functional effects. The present report includes experiments which cannot rule out a hydrophobic component required for the membrane effects but numerous reports describe cation effects on mitochondria induced by positive charges probes such as the results presented by Hoke *et al.* (1988) with smaller synthetic gold probes, which suggest that these experimental results depend on compensation of different electrostatic charges (Valdivia *et al.*, 1983).

More specific chemical binding of artificial gold clusters has been demonstrated by Safer *et al.* (1982) using undecagold, avidin and biotin. The participation of the peripheral positive charges of gc 21+ on mitochondrial effects is demonstrated by results obtained with succinylated probes described by Reardon and Frey (1984). Discussion on the development of positively charged probes to detect negative charges on cell surfaces and macromolecular systems is presented by Danon *et al.* (1972). The influence of electrostatic surface potential on mitochondrial oxidative phosphorylation is studied by Schafer *et al.* (1975) by monitoring the development of "energized state" of the membrane and movement out of protons utilizing chromophoric or fluorophoric probes. Schafer and Rowohl-Quisthoudt (1975) present references and discussion on the molecular mechanisms involved in fluctuations of membrane potential, surface charges, surface potentials, gradients and ionic fluxes.

Functional alterations induced by undecagold cluster binding to isolated mitochondria

The increase in respiration of HBHM secondary to

non-penetrating cationic electron dense probes may be due to electric charges compensation on the outer surface of the outer mitochondrial membrane because it has been observed with all substrates (succinate, malate, glutarate, β -hydroxybutyrate, α -ketoglutarate, pyruvate malate etc.) with well-coupled heart and liver mitochondria, with 150 mM KCl medium and is not observed in uncoupled or broken mitochondria or LBHM. Our additional observations of gc 21+ induced permeability changes of calcium, protons, and potassium may be interpreted as a result of the displacements needed by the mechanisms of charge separation. The physiologic importance of these findings beyond the realm of the experimental situation with isolated and modified mitochondria depends on the possibility that the electric properties of mitochondria may fluctuate within metabolic states, be modified by regulatory hormonal or molecular effects, or by electrostatic charged biologic substance such as polyamines and other cations. These results strongly imply the presence in the outer mitochondrial membrane of well-coupled HBHM, of an electric dependent signal transduction system capable of regulating ionic fluxes and respiration.

The permeability changes of mitochondria have been studied in uncoupled mitochondria by Peng *et al.* (1977), in liver mitochondria after calcium additions by Siekevitz and Potter (1955), in calcium induced transition by Hunter *et al.* (1976) and in anoxic cardiac myocytes by Cheung *et al.* (1986) which have demonstrated the release of nucleotides by mitochondria. Siekevitz and Potter (1955) also describe release of adenine nucleotides by incubated liver mitochondria. These nucleotides have negative electrostatic charges and may bind gc 21+ and be responsible for the visualization of small osmiophilic structures on the surface of LBHM (see Figure 4), which may represent gc 21+ and probably gc 21+ complexes with nucleotides being released from the organelles.

The dependence of outer mitochondrial channels (porin channels) on electrostatic charges and electric voltage may be partially responsible for the mitochondria apparent permeability changes. Control of the mitochondrial porin channel by a number of positive and negative charges is described by Mirzabekov and Ermishkin (1989). More recently, several ion channels have been studied and identified to be in the inner mitochondrial membrane. Kinnally *et al.* (1991) suggest that the calcium transition described by Hunter *et al.* (1976) and by others, may explain the alterations of permeability produced by cationic molecules binding to the organelle. We interpret the results of gc 21+ and cationized ferritin on HBHM to be the result of neutralization of electric charges on the outer surface of the outer mitochondrial membrane which are observed in a low ionic medium and in a 150 mM KCl medium more prone to screen electrostatic charges; in both cases calcium-out proton-in fluxes are observed.

The experiments describing the effects of gc 21+ binding to light beef heart mitochondria (LBHM) demonstrate inhibition of LBHM respiration. LBHM have lower content of calcium than HBHM which may be due to permeability changes and the presence of swollen and

broken organelles. The importance of permeability changes and calcium loss may resemble the loss of calcium reported by Peng *et al.* (1977) by well coupled liver mitochondria when exposed to DNP. HBHM exposed to DNP show inhibition of respiration when exposed to gc 21+; see Figure 2. Mitochondrial calcium efflux has been demonstrated in experimental induction of mitochondrial membrane damage and in matrix accumulation of some cations (Chavez *et al.*, 1987).

We believe that both morphologic and functional changes produced by gc 21+ binding to mitochondria are not specific but dependent on the electrostatic charges of the organelle and of the probe. It is possible that gc 21+ may penetrate the organelle if tests are prolonged and the mitochondria survive. Smaller cations such as artificial smaller gold probes produce similar functional effects (Hoke *et al.* 1988). Calcium, lead, polyamines and organic cations also induce mitochondrial functional effects which depend on electrostatic charges of the probes (Siekevitz and Potter, 1955; Chavez *et al.*, 1987); Cheung *et al.*, 1986; Coll *et al.*, 1982; Hatefi, 1985; Hunter *et al.*, 1976; Jacobus *et al.*, 1982; Lehninger *et al.*, 1978; Malmstrom and Carafoli, 1976; Peng *et al.*, 1977).

Alternative explanations are: excluded calcium induces uncoupling and increased permeability of the mitochondrial membranes, the changes in mitochondrial calcium activates the permeases which are needed for transfer of substrates, nucleotides, or another uncharacterized factor. Mechanisms and significance of mitochondrial calcium fluxes are discussed by Coll *et al.* (1982).

Electron microscope ultrastructure studies

Artificial clustered gold made to be polyvalent cations induce aggregation and morphologic changes on biological systems which have negative electrostatic charges. The principal aim of this study is to report the functional and morphologic changes induced by artificial clusters on mitochondria which are dependent on electrostatic charges for biologic activity. Compensation of peripheral charges explains readily the clumping observed in HBHM (Fig. 3), ETPH (Fig. 16) and bacterial pyruvate dehydrogenase (Fig. 5) after exposure to gc 21+.

Increase in the volume of matrix space (Fig. 3) of HBHM exposed to gc 21+ has been described in uncoupling by classic uncouplers such as dinitrophenol (Williams *et al.*, 1970; Munn, 1974), in the transition state induced by calcium (Hunter *et al.*, 1976), and in liver mitochondria (Hackenbrock, 1972). These changes may be explained by the chemiosmotic mechanisms of oxidative phosphorylation uncoupling as described by Mitchell (1966) and more recently reviewed by Hatefi (1985). We have mentioned previously the existence of outer mitochondria porin channels, and the description of inner mitochondrial calcium channels which may also be required for osmotic and ionic mitochondrial fluxes (Mirzabekov and Ermishkin, 1989; Kinnally *et al.*, 1991).

Gc 21+ induces apparent fusion of membranes in the LBHM, ETPH, and cytochrome oxidase preparations

which resemble the myelin membrane structures dependent on myelin basic protein (Rand *et al.*, 1979). These morphologies suggest the role of electrostatic positive charges on the formation of aggregated membrane systems which may lead to crystallization of organelles membrane structure (Henderson and Smith, 1980).

The osmiophilia of gc 21+ may lead to experimental tests of the mechanism required for binding of osmium and electron microscopy stain of biological structures. Our spectroscopic examination of suspensions of organelles, ETPH, cytochromes with and without gc 21+ (results not demonstrated) suggest that additional measurements may provide information on the molecular changes produced by gc 21+ and osmic acid involving redox and osmioamine reactions.

Visualization of individual gc 21+ particles is suggested in our examination of TEM electron micrographs above 150,000X magnification but such information is not required to explain our morphologic and functional results. Individual visualization of gc 21+ particles is observed in the dark field TEM examination. Dimerization or some aggregation can not be ruled out because of the thickness of the preparations.

Conclusions

1) Gc 21+ and cationic ferritin bind readily to the outside surface of isolated mitochondria. This experimental binding is dependent on negative electrostatic charges of mitochondria and positive electrostatic charges of the probes.

2) Binding of gc 21+ to membranes induces electric charge compensation which produces alterations of ion content and ion fluxes, and stimulation of electron transport in respiring, well-coupled heavy beef heart mitochondria.

3) The morphological changes observed by electron microscopy are secondary to the electrostatic charges of undecagold clusters and mitochondria.

Acknowledgements

This study has been supported by the following grants: University of Wisconsin Graduate School, University of Wisconsin Medical School, NIH grants GM-88, GM-12847, AM-32686, AM-28067, HE-06523, and CA-40445.

References

- Albano VG, Bellon PL, Manassero M, Sansoni M. (1970). Intermetallic pattern of metal-atom clusters. structural studies on $Au_{11}X_3$ (PR₃) species. Chem Comm 1210-1211.
- Balaban RS. (1990). Regulation of oxidative phosphorylation in the mammalian cell. Am J Physiol 258: C377-C389.
- Bartlett PA, Bauer B, Singer SJ. (1978). Synthesis of water-soluble undecagold cluster compounds of potential importance in electron microscopic and other studies

- of biological systems. *J Amer Chem Soc* **100**: 5085-5089.
- Blondin GA, Green DE. (1969). Mechanism of mitochondrial swelling. *Arch Biochem Biophys* **132**: 509-523.
- Brenner S, Horne RW. (1959). A negative staining method for high resolution electron microscopy of viruses. *Biochem Biophys Acta* **34**: 103-110.
- CaJacob CA, Frey PA, Hainfeld JF, Wall JS, Yang H. (1985). Escherichia coli pyruvate dehydrogenase complex: Particle masses of the complex and component enzymes measured by scanning transmission electron microscopy. *Biochemistry* **24**: 2425-2431.
- Cariati F, Naldini L. (1971). Trianionoeptakis (triarylphosphine)undecagold cluster compounds. *Inorgan Chim Acta* **5**: 172-174.
- Chance B, Williams GR. (1956). The respiratory chain and oxidative phosphorylation. *Adv Enzymol* **17**: 65-134.
- Chavez E, Jay D, Bravo C. (1987). The mechanism of lead-induced mitochondrial Ca^{2+} efflux. *J Bioenerget Biomembr* **19**: 285-295.
- Cheung JY, Leaf A, Bonventre JV. (1986). Mitochondrial function and intracellular calcium in anoxic cardiac myocytes. *Amer J Physiol* **250**: C18-C25.
- Coll KE, Joseph SK, Corkey BE, Williamson JR. (1982). Determination of the matrix free Ca^{2+} concentration and kinetics of Ca^{2+} efflux in liver and heart mitochondria. *J Biol Chem* **57**: 8696-8704.
- Crane FL, Glenn JL, Green DE. (1956). Studies on the electron transfer system. IV. The electron transfer particle. *Biochem Biophys Acta* **22**: 475-487.
- Danon D, Goldstein L, Marikovsky Y, Skutelsky E. (1972). Use of cationized ferritin as a label of negative charges on cell surfaces. *J Ultrastruct Res* **38**: 500-510.
- Erecinska M, Wilson DF. (1982). Regulation of cellular energy metabolism. *J Membr Biol* **70**: 1-14.
- Eskelinen S, Peura R. (1988). Location and identification of colloidal particles on the cell surface with a scanning electron microscope and energy dispersive analyzer. *Scanning Microscopy* **2**: 1765-1774.
- Fahien LA, Strmecki M, Smith S. (1969). Studies on gluconeogenic mitochondrial enzymes. *Arch Biochem Biophys* **130**: 449-455.
- From AHL, Zimmer SD, Michurski SP, Mohanakrishnan P, Ulstad VK, Thoma WJ, Ugurbil K. (1990). Regulation of the oxidative phosphorylation rate in the intact cell. *Biochemistry* **29**: 3731-3743.
- Gornall AG, Bardawill CJ, David MM. (1949). Determination of serum proteins by means of the biuret reaction. *J Biol Chem* **177**: 751-766.
- Gregory DW, Pirie BJS. (1973). Wetting agents for biological electron microscopy. *J Microsc* **99**: 251-265.
- Hackenbrock CR. (1972). Energy-linked ultrastructural transformations in isolated liver mitochondria and mitoplasts. *J. Cell Biol.* **53**: 450-465.
- Hainfeld JF. (1987). A small gold-conjugated antibody label: Improved resolution for electron microscopy. *Science* **236**: 450-453.
- Hansen M, Smith AL. (1964). Studies in the mechanism of oxidative phosphorylation. VII. Preparation of a submitochondrial particle (ETP) which is capable of fully coupled oxidative phosphorylation. *Biochem Biophys Acta* **1**: 214-222.
- Hatefi Y. (1985). The mitochondrial electron transport and oxidative phosphorylation system. *Ann Rev Biochem* **54**: 1015-1069.
- Heineman FW, Balaban RS. (1990). Control of mitochondrial respiration in the heart *in vivo*. *Annual Rev Physiol* **52**: 523-542.
- Henderson R, Smith D. (1980). Crystallization of purple membrane in three-dimensions. *J Mol Biol* **139**: 99-109.
- Hoke GD, Rush GF, Bossard GE, McArdle JV, Jensen BD, Mirabelli CK. (1988). Mechanism of alterations in isolated rat liver mitochondrial function induced by gold complexes of bidentate phosphines. *J Biol Chem* **263**: 11203-11210.
- Hoppeler H. (1990). The different relationship of $V_{Oxygen\ max.}$ to muscle mitochondria in humans and quadrupedal animals. *Resp Physiol* **80**: 137-146.
- Hunter DR, Haworth RA, Southard JH. (1976). Relationship between configuration, function and permeability in calcium-treated mitochondria. *J Biol Chem* **251**: 5069-5077.
- Jacobus WE, Moreadith RW, Vandegaer KM. (1982). Mitochondrial respiratory control. *J Biol Chem* **257**: 2397-2402.
- Kinnally KW, Zorov D, Antonenko Y, Perini S. (1991). Calcium modulation of mitochondrial inner membrane channel activity. *Biochem Biophys Res Comm* **176**: 1183-1188.
- Kuhn E, Fuchs M, Varkey J, Beer M, Yang HC, Frey P. (1984). Labeling of macromolecular assemblies with undecagold clusters. *Proceedings of the 42nd Annual Meeting of the Electron Microscopy Society of America*, San Francisco Press, San Francisco, pp 160-161.
- Lardy HA, Wellman H. (1953). The catalytic effect of 2,4-Dinitrophenol on adenosinetriphosphate hydrolysis by cell particles and soluble enzymes. *J Biol Chem* **210**: 357-370.
- Lehninger AL, Vercesi A, Bababunmi EA. (1978). Regulation of Ca^{2+} release from mitochondria by the oxidation-reduction state of pyridine nucleotides. *Proc Natl Acad Sci USA* **75**: 1690-1694.
- Lehninger AL. (1970). *Biochemistry. The molecular basis of cell structure and function*. Worth Publishers Inc., New York, pp 395-405.
- Lipka JJ, Hainfeld JF, Wall JS. (1983). Undecagold labeling of a glycoprotein: STEM visualization of an undecagold-phosphine cluster labeling the carbohydrate sites of human haptoglobin-hemoglobin complex. *J Ultrastruct Res* **84**: 120-129.
- Löw H, Vallin I. (1963). Succinate-linked diphosphopyridine nucleotide reduction in submitochondrial particles. *Biochem Biophys Acta* **69**: 361-374.
- Malmstrom K, Carafoli E. (1976). The effect of Ca^{2+} on the oxidation of β -hydroxybutyric acid by heart mitochondria. *Biochem Biophys Res Comm* **69**: 658-664.
- Mirzabekov TA, Ermishkin LN. (1989). The gate

- of mitochondrial porin channel is controlled by a number of negative and positive charges. *FEBS Lett* **249**: 375-378.
- Mitchell P. (1966). *Chemiosmotic Coupling in Oxidative in Oxidative and Photosynthetic Phosphorylation*. Glynn Res Ltd, Bodmin, Cornwall, England, pp 120-121.
- Moreno-Sanchez R, Hogue BA, Hansford RG. (1990). Influence of NAD-linked dehydrogenase activity on flux through oxidative phosphorylation. *Biochem J* **268**: 421-428.
- Munn EA. (1968). On the structure of mitochondria and the value of ammonium molybdate as a negative stain for osmotically sensitive structures. *J Ultrastruct Res* **25**: 362-380.
- Munn EA (1974). *The Structure of Mitochondria*. Academic Press, New York, pp 205-206.
- Murthy L, Menden EE, Eller PM, Petering HG. (1973). Atomic absorption determination of zinc, copper, cadmium, and lead in tissues solubilized by aqueous tetramethylammonium hydroxide. *Anal Biochem* **53**: 365-372.
- Muscatello U, Horne RW. (1968). Effect of the tonicity of some negative-staining solutions on the elementary structure of membrane-bounded systems. *J Ultrastruct Res* **25**: 73-83.
- Palade G.E. (1952). The fine structure of mitochondria. *Anat Rec* **114**: 427-451.
- Pease, D.C. (1964). *Histological Techniques for Electron Microscopy*. 2nd ed. Academic Press, New York, pp 236-237.
- Peng CF, Straub KD, Kane JJ, Murphy ML, Wadkins CL. (1977). Effects of adenosine nucleotide translocase inhibitors on dinitrophenol induced Ca^{2+} efflux from pig heart mitochondria. *Biochem Biophys Acta* **462**: 403-413.
- Rand RP, Fuller NL, Lis LJ. (1979). Myelin swelling and measurement of forces between myelin membranes. *Nature* **279**: 258-260.
- Reardon JE, Frey PA. (1984). Synthesis of undecagold cluster molecules as biochemical labeling reagents. I. Monoacyl and mono [N-(succinimido-oxy)succinyl] undecagold clusters. *Biochemistry* **23**: 3849-3856.
- Reed PW, Lardy HA. (1972). A23187: A divalent cation ionophore. *J Biol Chem* **247**: 6970-6977.
- Rzeczycki W, Valdivia E. (1973). Mitochondria uncoupling effect of halothane dependent on magnesium. *Biochem Biophys Res Comm* **52**: 270-275.
- Safer D, Hainfeld J, Wall JS, Reardon JE. (1982). Biospecific labeling with undecagold visualization of the biotin site on avidin. *Science* **218**: 290-291.
- Safer D, Bolinger L, Leigh Jr JS. (1986). Undecagold clusters for site-specific labeling of biological macromolecules: Simplified preparation and model applications. *J Inorgan Biochem* **26**: 77-91.
- Schafer G, Rowohl-Quisthoudt G. (1975). Influence of electrostatic surface potential on mitochondrial ADP-phosphorylation. *FEBS Lett* **59**:48-51.
- Siekevitz P, Potter VR. (1955). Biochemical structure of mitochondria. *J Biol Chem* **215**: 221-235.
- Sumegi B, Freeman DA, Inman L, Srere PA. (1988). Studies on a possible molecular basis for the structure of mitochondrial cristae. *J Mol Recog* **1**:19-24.
- Sun FF, Prezbindowski KS, Crane FL, Jacobs EE. (1968). Physical state of cytochrome oxidase, relationship between membrane formation and ionic strength. *Biochem Biophys Acta* **153**: 804-818.
- Tandler B, Hoppel CL. (1972). *Mitochondria*. Academic Press, New York, pp 31-33.
- Valcarce C, Vitorica J, Satrustegui J, Cuezva JM. (1990). Rapid postnatal developmental changes in the passive proton permeability of the inner membrane in rat liver mitochondria. *J Biochem* **108**: 642-645.
- Valdivia E, Watson M, Dass CMS. (1960). Histologic alterations in muscles of guinea pigs during chronic hypoxia. *Arch Pathol* **69**: 199-208.
- Valdivia E, Pease B, Gabel C, Chan V. (1973). Electrophoresis of isolated mitochondria. *Anal Biochem* **51**: 146-151.
- Valdivia E, Gabel C, Reardon JE, Frey PA. (1983). Synthetic gold cluster binding to isolated mitochondria. *Fed Proc* **42**: 1278 (abstr).
- Wall JS. (1978). Limits on visibility of single heavy atoms in the scanning transmission electron microscope - An experimental study. *Chem Scripta* **14**: 271-278.
- Wall JS, Hainfeld JF, Bartlett PA, Singer SJ. (1982) Observation of an undecagold cluster compound in the scanning transmission electron microscope. *Ultramicroscopy* **8**: 397-402.
- Williams CH, Vail WJ, Harris RA, Caldwell M, Green DE, Valdivia E. (1970). Conformational basis of energy transduction in membrane systems. VIII. Configurational changes of mitochondria *in situ* and *in vitro*. *Bioenergetics* **1**: 147-180.
- Yang H, Reardon JE, Frey PA. (1984). Synthesis of undecagold cluster molecules as biochemical labeling reagents. 2. Bromoacetyl and maleimido undecagold clusters. *Biochemistry* **23**: 3857-3862.
- Yang H, Frey PA. (1984). Synthesis of undecagold cluster molecules as biochemical labeling reagents. 3. Dimeric cluster with a single reactive amino group. *Biochemistry* **23**: 3863-3868.

Discussion with Reviewers

J.F. Hainfeld: The gold cluster is somewhat hydrophobic due to its phenyl groups and it adheres to reverse phase material. Can you rule out its attachment to membranes by this type of interaction?

Authors: We cannot rule out completely that the attachment of gc 21+ to mitochondria has a hydrophobic component of interaction but we favor the electrostatic dependent effect to be responsible for most of the functional and morphological changes.

J.F. Hainfeld: In many of your preparations, you fix the samples with glutaraldehyde in a reasonably concentrated gc solution. The gc contains amines (21) and will be cross-linked to proteins. The outer surfaces are then claimed to be stained by ionic or specific attachment. Your experiments should wash excess gc out before fixing

to be able to make your conclusions.

Authors: We have done experiments which follow exactly your suggestions, measurements of gc 21+ binding to HBHM, LBHM and enzymatic systems present similar results before and after glutaraldehyde fixation. We believe that binding is fast to explain the absence of differences.

J.F. Hainfeld: You use various microscopes and conditions to try to see gc's. According to Wall *et al.* (1982) the undecagold loses mass with electron dose and quickly becomes invisible.

Authors: The method used by Wall *et al.* is valid for their conditions and microscopy but it cannot be applied to our experiments with fixed and embedded material. Furthermore we believe that the sites of binding are crosslinked which apparently makes the gc 21+ more stable since in TEM electron dense images appear to persist at 100 kV.

J.F. Hainfeld: What doses did you use for imaging, and how much loss do you predict?

Authors: We did not measure electron doses, the results described above and in the text refer to Hitachi model 11E and JEOL CX at 100 kV. We do not know if there is matter loss in our experiments. In the dark field experiments we saw no loss of apparent gc 21+ material for at least 5 minutes of observations.

J.F. Hainfeld: What was the resolution in nm of the energy dispersive X-ray image?

Authors: We used a JEOL CX microscope in the scanning mode, 100 kV and a window of approximately 20×10^6 square Ångströms.

J.F. Hainfeld: You claim that single gc's can be seen in Fig. 5. Although there are obvious spots probably due to gold, they vary in size and many appear on the background unexpectedly unattached to the protein. It is therefore unclear whether single cluster visibility can be claimed from this experiment. Please comment.

Authors: This is darkfield method obtained with the manufacturer's instructions of JEOL 100CX. We concur with your statements: resolution of the test structures is naturally poor but certainly the bright spots are probably due to the higher density of the gold cluster, but superimposition, closeness and double presence may explain the results obtained.